ELSEVIER

Ceramics International 25 (1999) 317–324

CERAMICS INTERNATIONAL

Evaluation of CaO–CeO_2–partially stabilized zirconia thermal barrier coatings

Parvati Ramaswamy [a], S. Seetharamu [a], K.B.R. Varma [b], K.J. Rao [b,*]

[a] *Materials Technology Division, Central Power Research Institute, Bangalore, India*
[b] *Materials Research Centre, Indian Institute of Science, Bangalore, India*

Received 2 October 1997; accepted 16 March 1998

Abstract

Plasma sprayable powders were prepared from ZrO_2–CaO–CeO_2 system using an organic binder and coated onto stainless steel substrates previously coated by a bond coat (Ni 22Cr 20Al 1.0Y) using plasma spraying. The coatings exhibited good thermal barrier characteristics and excellent resistance to thermal shock at 1000°C under simulated laboratory conditions (90 half hour cycles without failure) and at 1200°C under accelerated burner rig test conditions (500 2 min cycles without failure). No destabilization of cubic/tetragonal ZrO_2 phase fraction occured either during the long hours (45 h cumulative) or the large number of thermal shock tests. Growth of a distinct SiO_2 rich region within the ceramic was observed in the specimens thermal shock cycled at 1000°C apart from mild oxidation of the bond coat. The specimens tested at 1200°C had a glassy appearance on the top surface and exhibited severe oxidation of the bond coat at the ceramic–bond coat interface. The glassy appearance of the surface is due to the formation of a liquid silicate layer attributable to the impurity phase present in commercial grade ZrO_2 powder. These observations are supported by SEM analysis and quantitative EDAX data.

Keywords: C. Thermal shock resistance; Thermal barrier coating; Partially stabilized zirconia; Plasma spray

1. Introduction

ZrO_2, partially stabilized with CaO, MgO or Y_2O_3 is the most extensively studied system for thermal barrier applications. They are generally plasma sprayed onto metal substrates and these thermal barrier coatings (TBCs) exhibit very low thermal conductivity, medium thermal expansion and high thermal shock resistance characteristics. The commonly used TBCs are stabilized zirconias with CaO (5 wt%) [1], MgO (15–24 wt%) [2] and Y_2O_3(6–12 wt%) [3–5]. Among them, MgO–ZrO_2 is the most difficult to plasma spray coat because of its tendency to vaporise at elevated temperatures [2]. Twenty-four percent MgO–ZrO_2 is known to exhibit destabilization of c-ZrO_2 to m-ZrO_2 when exposed to temperatures above 950°C [2]. This degradation reaction results in an increase in its thermal conductivity as well as structural disintegration. CaO–ZrO_2 compositions also show poor stability with respect to spraying parameters [6,7]. Five percent CaO–ZrO_2 coatings on turbine blades of a modified cyclic jet engine were subjected to thermal cycling between 1077°C and ~577°C. At the end of 500 2-min cycles they were found to develop microcracks [1]. Most desirable thermomechanical properties are exhibited by ZrO_2 stabilized with 8% Y_2O_3 [2]. The tetragonal phase formed in this composition is stable up to 1400°C. Generally, compositions in this system are stable with respect to spraying parameters. They also exhibit excellent thermal shock and thermal barrier characteristics which are superior to those of CaO-stabilized ZrO_2 coatings [1,7]. In addition to the above stabilizers, all the rare earth oxides are also found to 'stabilize' the cubic flourite structure of ZrO_2; whereby the cubic → tetragonal transformation occurs at a lower temperature. Among the rare earth doped partially stabilized zirconia (PSZ), zirconia–ceria (ZrO_2–CeO_2) alloys are considered to be promising alternatives to zirconia stabilized with 6–8 wt% Y_2O_3 [8–10]. This is because CeO_2 provides partial stabilization of ZrO_2 over a wide range of compositions (e.g. 5 to 85 wt% of CeO_2 at 1200°C) and also exhibits a lower

* Corresponding author.

0272-8842/99/$20.00
PII: S0272-8842(98)00041-8

thermal conductivity, higher toughness and thermal shock resistance compared to plasma sprayed ZrO_2–Y_2O_3 coatings [8,10]. However, CeO_2 tends to reduce to Ce_2O_3 during spraying of ceria-stabilized zirconia, leading to the formation of a metastable phase. The equilibrium stoichiometry can be reached after a low temperature annealing in air which results in restoration of polymorphic phase concentration. This influences the mechanical properties and stability of the coatings [11]. Further, a redox-reaction has been reported to occur in a ceria–zirconia sintered system when about 1 wt% silica (SiO_2) impurity is present. The reaction is triggered at temperatures above 1200°C [12] and results in the formation of a liquid 'silicate' film either at grain boundaries, in large pores or on the surface.

Efforts have been made during the last decade to optimize the chemistry of zirconia based TBCs. Preparation of coatings using different stabilizers, use of a variety of process parameters and modifications of outer layer surface have been examined in this context [13,14]. Recently, a combination of CeO_2 and Y_2O_3 has also been used as stabilizer in ZrO_2 TBCs [8]. An investigation of the effectiveness of multiple stabilizers in ZrO_2 is in order. We have therefore examined use of commercial grade ZrO_2 stabilized with a combination of CaO, CeO_2 and MgO as TBCs. Plasma sprayable powders of ZrO_2 were made using CaO [15], and CeO_2 was added as additional stabilizer. Since MgO was used as a processing aid, the present TBC consists of CaO, MgO and CeO_2. It also contains a small proportion of SiO_2 which is present as an impurity. The focus in this work is to study the effect of the combination of stabilizers on thermal shock and thermal barrier properties, phase stability and microstructural aspects.

2. Experimental procedures

2.1. Powder preparation

The raw materials were of commercial grade zirconia (ZrO_2, ~99.0%, SiO_2, ~1%), and ceramic grade magnesium oxide (MgO, 99.9%), calcium oxide (CaO, 99.9%) and cerium oxide (CeO_2, 99.9%). The composition in wt% was 93.2% ZrO_2, 3.2% CeO_2, 3.4% CaO and 0.2% MgO. The raw material powders were ground wet in agate ball mill, dried and calcined at 1150°C for 12 h in air. The calcined powder was heated further to a higher temperature of about 2000°C using an oxy-acetylene torch in order to ensure complete homogenization of stabilizing oxides in ZrO_2. The resulting fine particles whose composition is designated as ZCC was made into plasma sprayable powder by granulating them with an organic binder. The details of the preparation of plasma sprayable powder is described elsewhere [15].

2.2. Spray coated specimen preparation

Stainless steel substrates were used for preparation of spray coated specimens. 100×100×3 mm stainless steel substrates were first coated with 100 μm thick bond coat material (AMDRY 962, designated NiCrAlY in the present work). This was followed by a spray coat of the ZCC plasma sprayable powder to a thickness of 275 μm. These experimental specimens are designated as ZCC (as-sprayed). Typical spray parameters are given in Table 1.

2.3. Characterization

2.3.1. Phase analysis and microstructure

Qualitative and quantitative phase analyses were carried out using X-ray diffractometry (XRD) with CuK_α radiation. Scanning electron microscopy (SEM) associated with energy dispersive X-ray analysis (EDAX) was employed to study the microstructural details and to determine quantitative elemental composition.

2.3.2. Thermal shock and thermal barrier tests

In order to study the thermal shock behaviour, the coatings were subjected to two types of thermal shock cycles: (i) long cycle and (ii) short cycle. The long cycle consisted of suddenly exposing the ceramic side of the coating to an oxy-acetylene flame. The flame temperature on the ceramic surface was maintained at 1000 ± 10°C for 30 min, and the flame was quickly withdrawn, and the specimen cooled using a fan such that the surface temperature of the coating was brought down to < 100°C within 30 s. (ii) The short cycle consisted of a standard test [1,15] under accelerated conditions in a cyclic burner rig using aviation fuel flame. It is routinely employed to evaluate thermal shock properties under severe thermal conditions and environment. The short cycle tests in the present work comprised of sudden heating of the ceramic surface to 1200 ± 10°C in the burner rig flame, soaking in the flame for 60 s at the same temperature, withdrawal from the flame for 60 s

Table 1
Plasma spray parameters

Argon flow rate	44 L/min
Hydrogen flow rate	13 L/min
Powder gas flow rate	3.4 L/min
Current	600 amps
Voltage	70 volts
Nozzle/electrode diameter	6 mm
Injector diameter	1.8 mm
Injector angle	90°
Injector distance	6 mm
Powder feed rate	40 (gm/min)
Spray distance	120 mm

The substrate was kept air cooled during spraying.

during which time the metal temperature came down to $<200°C$ and repeat the cycle. Extensive microcracking was known to occur in $CaO–ZrO_2$ sintered systems when it was thermal shock cycled with a temperature gradient ΔT, of 1100°C. The incidence of microcracking is attributed to t → m phase transformation within the subgrains of pure ZrO_2 present in cubic ZrO_2 matrix [16,17]. The short cycle thermal shock test was designed to respond sensitively to the effect of any such kinetically controlled phase transformations. Both the tests were carried out on two samples each.

The temperature on the ceramic surface and the metal was measured by using K-type (chromel–alumel) thermocouple and optical pyrometer. Proper thermal contacts of the thermocouple were ensured by cementing the thermocouple junction to the ceramic by high temperature conducting Ag–Pd paste. The temperature drop across the ceramic coating was determined by measuring the temperature of the metal when the ceramic surface was at 1000°C. These measurements were made only after the system attained steady state. The samples were subjected to 90 long and 500 short thermal shock cycles. They are designated as ZCC 90 and ZCC 500, respectively, in the following discussion.

3. Results and discussion

Fig. 1 shows the scanning electron micrograph of the ZCC powders (non-sprayable). The particles are smooth with rounded edges due to the near melting temperature attained during their preparation. The particle size ranges from 3–10 μm. The scanning electron micrograph of sprayable powder is shown in Fig. 2. Very clearly these particles are agglomerates of 50–120 μm size and are formed from the ZCC particles of Fig. 1.

The X-ray diffractogram of the sprayable powder is shown in Fig. 3. The diffraction patterns of as-sprayed and thermal shock tested specimens are also included in the figure. The sprayable powder consisted of two phases namely cubic/tetragonal zirconia (c/t-ZrO_2) and monoclinic zirconia (m-ZrO_2). The phase fractions of m-ZrO_2 and c/t-ZrO_2 were determined by Polymorph technique [18], in which $X_{c/t}$, the phase fraction of c/t ZrO_2 is given by $X_{c/t} = I_{c/t(111)}[1/(I_{m(111)} + I_{m(11\bar{1})} + I_{c/t(111)})]$ where I_m and $I_{c/t}$ are the intensities of the

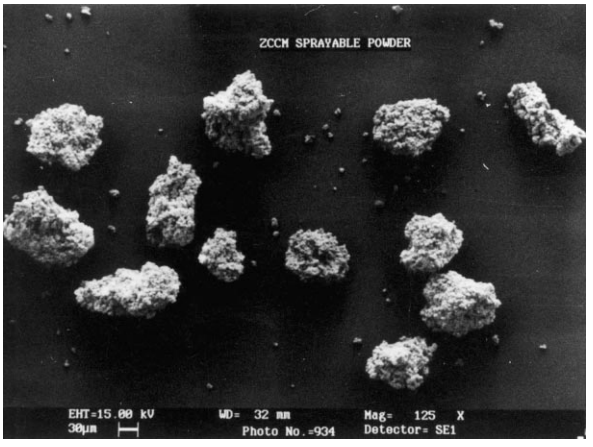

Fig. 2. Scanning electron micrograph of ZCC powder (sprayable).

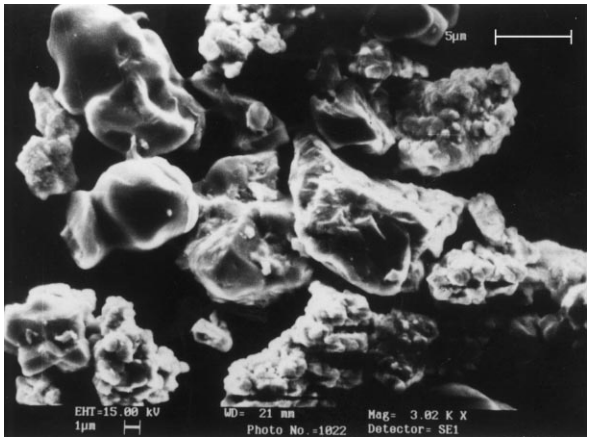

Fig. 1. Scanning electron micrograph of ZCC powder (non-sprayable).

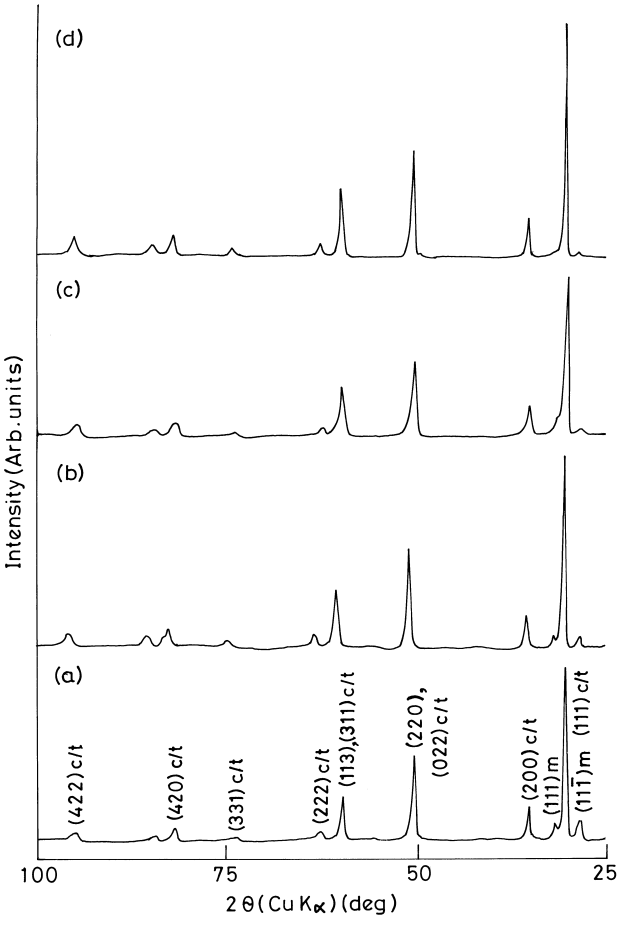

Fig. 3. X-ray diffractograms of (a) ZCC powder (sprayable), (b) ZCC (as-sprayed), (c) ZCC 90 and (d) ZCC 500.

reflections corresponding to the monoclinic and cubic/tetragonal phases, respectively.

No efforts have been made in the present work to deconvulate the overlapping c/t-ZrO_2 peaks. The percentage of c/t-ZrO_2 phase fraction for all the patterns presented in Fig. 3 is given in Table 2. Partial stabilization (84.6%) of the c/t-ZrO_2 phase is evident in the sprayable powder.

The ZCC (as-sprayed) specimens were orangish yellow typically due to the presence of cerium in 3+ oxidation state. They turned white immediately on exposure to temperatures >1000°C during thermal shock cycle tests because of the change in oxidation state of cerium from Ce^{3+} to Ce^{4+} [19].

The sprayed surface had a R_a value (Roughness average: arithmetic mean deviation of roughness profile) of 8.03 μm. The specimens exhibited excellent thermal shock resistance in both long and short cycle tests. The coatings were intact without any evidence of detachment from the substrate after the tests. It may be recalled that 5% CaO–ZrO_2 coatings were earlier found to develop microcracks when thermal shock cycled even with smaller temperature gradient ($\Delta T \simeq 500$°C) and with a lower ceramic temperature (1077°C) compared to the present work [1]. We have confirmed that the 5% CaO–ZrO_2 coating behave in the same reported manner by plasma spraying a powder of that composition (prepared by binder method [15]) and subjecting the sprayed sample to accelerated burner rig short cycles test (unpublished work). The 5% CaO–ZrO_2 coatings withstood only 380 thermal shock cycles before spallation of the ceramic overcoat occured in the burner rig test. Therefore, the present study confirms the superior thermal shock resistance (TSR) of ZrO_2–CaO–CeO_2 composition compared to ZrO_2–CaO composition. There is thus a positive effect of CeO_2 which improves the TSR properties of ZrO_2–CaO coatings.

We have observed earlier that 8% Y_2O_3–ZrO_2 composition also showed no detachment of the coatings from the substrate when subjected to identical process and test conditions even at the end of 500 short cycles [unpublished work]. Further, ZCC (as-sprayed) registered a temperature drop (ΔT) of 240°C across the coating when the ceramic surface was maintained at a temperature of 1000°C. Even 5% CaO–ZrO_2 coatings were found to exhibit similar thermal barrier characteristics ($\Delta T = 200$°C) (unpublished work). Therefore, ZCC coatings were found to have similar TBC characteristics as the 8% Y_2O_3–ZrO_2 and 5% CaO–ZrO_2 coatings. The photographs of (a) ZCC (as-sprayed) and (b) ZCC 500 are shown in Fig. 4.

Table 2
Percentage phase fraction (c/t-ZrO_2 and m-ZrO_2)

Sl no.	Specimen	% c/t-ZrO_2	% m-ZrO_2
1	ZCC (sprayable powder)	84.6	15.4
2	ZCC (as-sprayed)	91.0	9.0
3	ZCC-90	95.0	5.0
4	ZCC-500	>95.0	<5.0

The process of spray coating seems to further stabilize the c/t-ZrO_2 phase in the sprayable powder from 84.6 to 91% (Table 2). No destabilization of the c/t-ZrO_2 phase was seen to occur on thermal shock cycling. In fact, the test process appears to lead to even higher levels of stabilization of the c/t phase of ZrO_2 (95+%). The phase stability of the coatings exposed to both the 1000°C long cycle test (45 h of cumulative exposure) and the 1200°C cycle test (500 min of cumulative exposure) is thereby confirmed.

Fig. 5 shows the scanning electron micrographs of the cross-section of (a) ZCC (as-sprayed), (b) ZCC 90 and (c) ZCC 500. The summary of the quantitative EDAX data of various regions in the cross section and the surface are given in Table 3. The smooth interface (Fig. 5a) suggests the existence of good bonding at the junctions of the ceramic, bond coat and the substrate. It is evident from the EDAX data that the bond coat contains a small amount of oxygen (7.11%) and the ceramic overlayer has about 1.63% of SiO_2. It may be noted that since the spraying process was carried out in air, the bond coat must have been slightly oxidised during the spray coating. SiO_2 originates as an impurity phase present in ZrO_2. It is also possible that SiO_2 is introduced during the ball-milling in agate grinding jars and balls.

The cross section of ZCC 90 (Fig. 5b) revealed an interesting feature within the ceramic overcoat (marked by an arrow). It consists of grains of strikingly different morphology from the rest of the coating. A closer view of this region is shown as the inset of Fig. 5b. These observations are corraborated by a detailed quantitative EDAX analysis (Table 3). These data may throw light on the possible mechanism of failure which eventually occurs on further shock cycling. A distinct SiO_2–Al_2O_3–CaO matrix/region (SiO_2 ~62.54%, CaO ~22.23% and Al_2O_3 ~14.73%) containing round and oval shaped

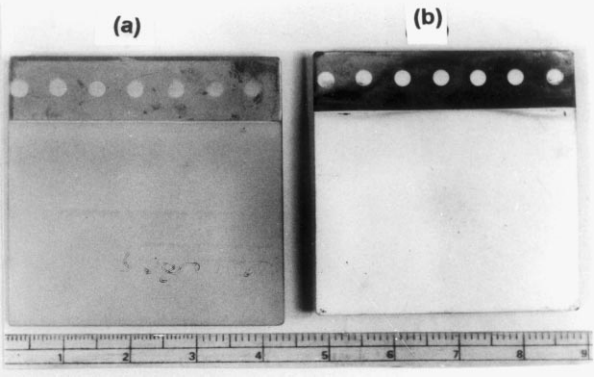

Fig. 4. Photograph of (a) ZCC (as-sprayed) and (b) ZCC 500.

Table 3
EDAX (quantitative analysis) data

Composition before thermal shock cycling (ZCC as-spray)

Bond coat (element %)		Ceramic (oxide %)	
Ni	61.96	ZrO_2	93.34
Cr	20.10	CaO	3.67
Al	10.83	MgO	0.23
O	7.11	Ce_2O_3	1.13
		SiO_2	1.63

Composition after thermal shock cycling at 1000°C (ZCC 90)

Bond coat (element % near ceramic)		Ceramic (oxide %)		Matrix (oxide %)		Precipitates (oxide %)	
Ni	51.40	ZrO_2	93.68	ZrO_2	–	ZrO_2	11.53
Cr	17.39	CaO	2.67	CaO	22.23	CaO	18.07
Al	15.30	MgO	0.22	MgO	0.50	MgO	–
O	14.95	CeO_2	3.10	CeO_2	–	CeO_2	1.00
Ca	0.13	SiO_2	0.33	SiO_2	62.54	SiO_2	55.56
Fe	0.83	Al_2O_3	–	Al_2O_3	14.73	Al_2O_3	13.84

Composition after thermal shock cycling at 1200°C (ZCC 500)

Bond coat (element%)			Ceramic (oxide %)		
Element	Near substrate	Near ceramic	Oxide	Near bond coat	Near surface
Ni	57.97	41.73	ZrO_2	89.93	84.25
Cr	21.27	17.29	CaO	2.06	5.39
Al	12.89	20.19	MgO	0.25	0.45
O	7.87	20.79	CeO_2	1.02	3.28
			SiO_2	1.57	6.22
			Al_2O_3	5.17	0.41

SiO_2 rich precipitates (SiO_2 ~55.56%) with significant amount of Al_2O_3 (13.84%), ZrO_2 (11.53%) and CaO (18.07%) was observed within the ceramic overlayer close to the bond coat–ceramic interface. The width of this distinct region is about 30 μm. The SiO_2 content in the ceramic overlayer near the bond coat is distinctly less (0.33%) suggesting that the concentration of SiO_2 at the particular region may be due to migration of Si ions towards the surface of the coating. The bond coat appeared to be more oxidised as compared to ZCC (as-sprayed) with an increased oxygen content of 14.95% near the ceramic interface. Cracks were also observed in the microstructure of the interface region. The formation of the distinct region consisting of SiO_2–Al_2O_3–CaO layer would probably lead to eventual failure of the coating upon further shock cycling. However, no major cracks were observed in the ceramic overlayer on either side of the compositionally distinct region.

The ceramic–bond coat–substrate interface in ZCC 500 (Fig. 5c) is not smooth and EDAX analysis (Table 3) gave evidence for both (i) oxidation of the bond coat and (ii) the presence of Al_2O_3 at the ceramic–bond coat interface. While the bond coat region near the substrate and the ZCC (as-sprayed) contained similar amounts of oxygen (7.87%), a higher oxygen content (20.79%) was recorded at the ceramic interface. The ceramic near the bond coat region contains 5.17% Al_2O_3 but there was a depletion of CaO and ZrO_2 from this layer. The formation of Al_2O_3 in this region is probably due to the oxidation of Al in the bond coat. The mechanism of oxidation of bond coat and the growth of Al_2O_3 grains at the interface has been reported in the literature [20–22]. However, unlike in earlier cases [20], no evidence of NiO rich Ni $(Cr,Al)_2O_4$ spinels was observed on the interface. Absence of cracks on the ceramic in spite of shock cycling with a large temperature gradient ($>1000°C$) confirms the excellent thermal shock resistance of the present ceramic composition. No depletion in either MgO, CaO or CeO_2 contents was observed in the ceramic overlayer in the region away from the bond coat.

Fig. 6 shows the scanning electron micrographs of the surface of (a) ZCC (as-sprayed), (b) ZCC 90 and (c) ZCC 500. As-sprayed coating reveals a fine grained microstructure with some amount of porosity, typical of plasma sprayed ceramics. Although the grain size in the sprayable powder was found to be between 50–120 μm (Fig. 2), the sub grains constituting the particles were

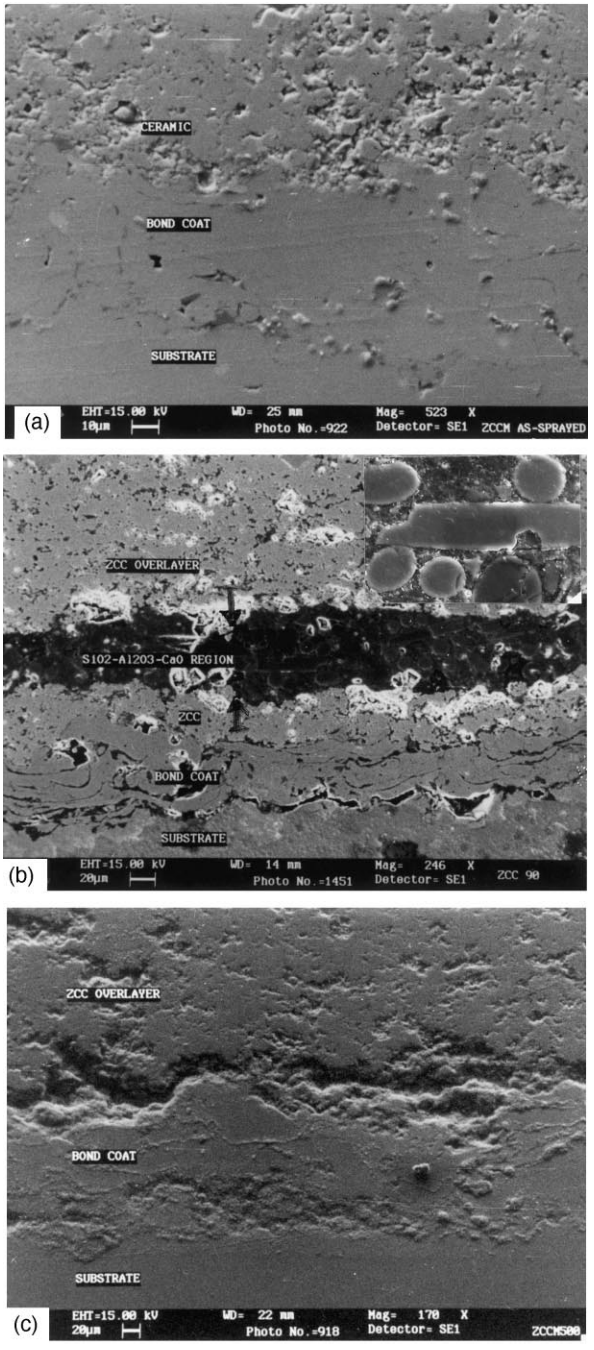

Fig. 5. Scanning electron micrographs of the cross-section of (a) ZCC (as-sprayed), (b) ZCC90 (inset: SiO_2 rich precipitates) and (c) ZCC 500.

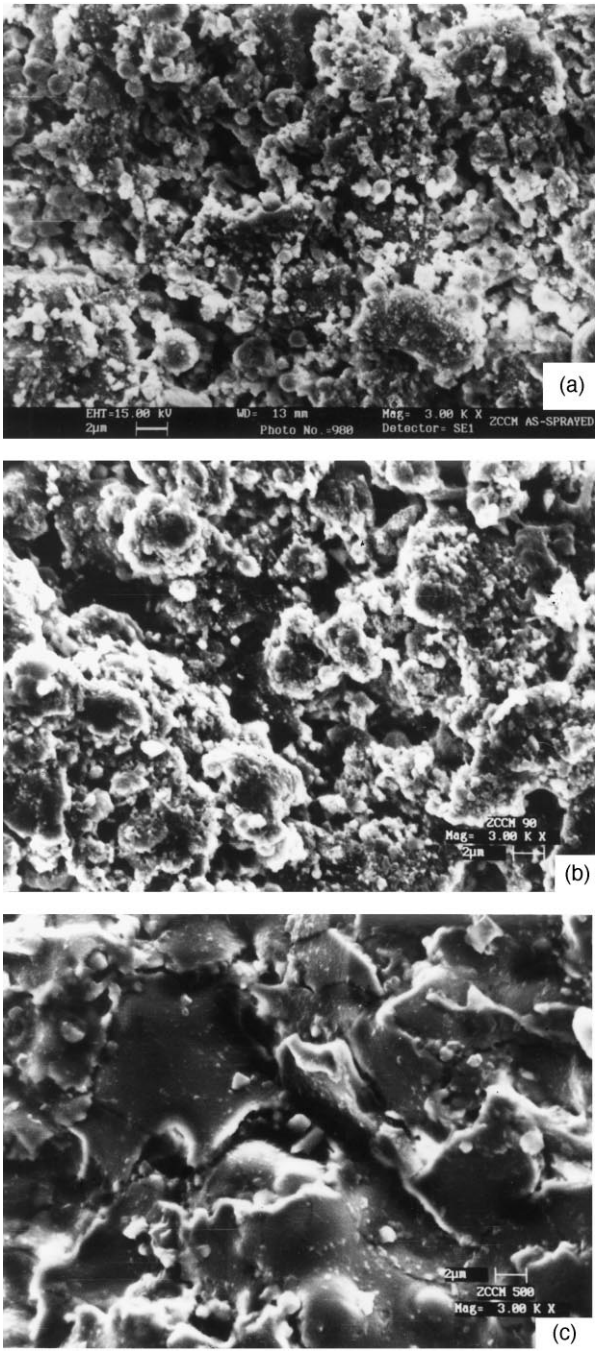

Fig. 6. Scanning electron micrographs of the surface of (a) ZCC (as-sprayed), (b) ZCC 90 and (c) ZCC 500.

only 3–10 μm (Fig. 1) and this is reflected in the surface morphology of ZCC (as-sprayed) specimen. The microstructure of the surface of ZCC 90 (Fig. 6b) is similar to that of the as-sprayed surface (Fig. 6a) except for grain growth and clustering of grains along with more porous structure. ZCC 500 (Fig. 6c) exhibited a rather different surface topography as compared with ZCC (as-sprayed) and ZCC 90 (Fig. 6a, b). The surface appeared smooth (typical of liquid phase formation), significantly less porous and indicated excessive grain growth. This may be a consequence of the high temperature used for the test (1200°C). The chemical composition of the surface of the ceramic (Table 3) analysed randomly to include both molten and some unaffected region indicated high concentration of MgO (0.45%), CaO (5.39%) and SiO_2 (6.22%) compared to original as-sprayed ceramic. It is very likely that a liquid silicate layer is formed which is compositionally a CaO–MgO–SiO_2 glass forming melt.

The melt has low viscosity due to the presence of efficient bond breakers like CaO and MgO. The grains of ZrO_2 ceramic are all swathed in the glass forming silicate melt. This type of surface has been observed only in ZCC 500 and the composition of the bulk of the ceramic below the surface layer remained unchanged except near the ceramic-bond coat interface (formation and segregation of Al_2O_3). Spot chemical analysis by EDAX on the smooth, large grains indicated the presence of large percentage of SiO_2 (~10–11%).

Scanning electron microscopy and EDAX analysis were performed on thermal shock cycled 5% $CaO–ZrO_2$ and 8% $Y_2O_3–ZrO_2$ coatings also. However, no SiO_2 rich glassy layers were observed in any region in spite of the fact that the as-sprayed specimens contained the same level of SiO_2 impurity. Thus, the formation of glassy SiO_2 rich layer seems to be present only when MgO is present. MgO-free coating of CeO_2 stabilized ZrO_2 also did not show any evidence of the formation of glassy layer. $MgO–SiO_2$ melts have a low viscosity and presence of MgO, CaO and small amounts of Al_2O_3 lower the liquidus temperatures and viscosities of silicate melts significantly [23]. Therefore, the interface between bond coat and the ceramic subjected to high temperature (low duration cycle) offers a recipe for the formation of $CaO–MgO–Al_2O_3–SiO_2$ glass forming melt of reduced viscosity which percolates and forms a smooth glassy coating on all the grains. During long duration-low temperature cycles the glassy layer is absent because the temperature is insufficient to form a low viscosity melt and the locally confined high viscosity melts form globules into which very small particles of other constituents like $CeO_2–ZrO_2$ also enter and globules simply freeze. The formation of such SiO_2 rich layers may also significantly affect the thermal barrier properties of the system by bringing about an increase in the thermal diffusivity of the ceramic. This aspect has not been studied in the present work. The TSR properties of $CaO–CeO_2–ZrO_2$ are most likely to be further improved when processed without the presence of SiO_2 in the system.

4. Conclusions

Plasma sprayed ceramic composition based on $ZrO_2–CaO–CeO_2$ system exhibits excellent thermal shock resistance which is superior to that of 5% $CaO–ZrO_2$ coatings. A temperature drop of 240°C was achieved across the thermal barrier coating at the metal substrate when the ceramic surface was at 1000°C. This result is comparable with that of 5% $CaO–ZrO_2$ coatings. The coating composition posseses very good phase stability even after 90 long thermal shock cycles between 1000°C and <100°C and 500 short thermal shock cycles between 1200 and <200°C. Although the specimens were not thermal shock cycled to failure, it is conjectured that the probable mode of eventual failure may be due to (i) the formation of a distinct SiO_2 rich region with high Al_2O_3 and CaO content in the ceramic close to the bond coat (in long duration thermal shock tests) and (ii) the oxidation of bond coat with growth of Al_2O_3 precipitates (in short duration thermal shock tests). The absence of an impurity phase SiO_2 in the ceramic coating is likely to further improve the thermal shock properties of the composition under investigation.

Acknowledgements

Two authors (PR and SS) thank the management of CPRI for permission to publish this paper. The burner rig test facilities were provided by the Gas Turbine Research Institute, Bangalore which is gratefully acknowledged.

References

[1] C.H. Liebert, R.E. Jacobs, S. Stecura, R.C. Morse, Durability of zirconia thermal barrier ceramic coatings on air-cooled Turbine blades in cyclic jet engine operation, TM X-3410, NASA, Washington, DC, 1976.
[2] A. Bennett, Properties of thermal barrier coatings, Mater. Sci. And Technol. 2 (1986) 257–261.
[3] J.R. Brandon, R. Taylor, Thermal properties of ceria and yttria partially stabilized zirconia thermal barrier coatings, Surface and Coatings Technology 39/40 (1989) 143–151.
[4] H.D. Steffens, U. Fischer, Characterization and thermal shock testing of yttria-stabilized zirconia coatings, Surface and Coatings Technology 32 (1987) 327–338.
[5] S. Alperine, L. Lelait, Microstructural investigations of plasma sprayed yttria partially stabilized zirconia TBC (in relation to thermomechanical resistance and high temperature oxidation mechanisms), J. Engg. for Gas Turbines and Power, Trans ASME 116(1) (1994) 258–265.
[6] P. Vincenzini, Zirconia thermal barrier coatings for engine applications, Industrial Ceramics 10(3) (1990) 113–126.
[7] D.S. Suhr, T.E. Mitchell, R.J. Keller, Microstructure and durability of zirconia thermal barrier coatings, in: N. Claussen, M. Ruhle, A.H. Heuer (Eds.), Science and Technology of Zirconia II, Advances in Ceramics, Vol. 12, ACS, Columbus, OH, USA, 1984, pp. 503–517.
[8] R.D. Maschio, P. Scardi, L. Lutterotti, G.M. Ingo, Influence of Ce^{3+}/Ce^{4+} ratio on phase stability and residual stress field in ceria–yttria stabilized zirconia plasma-sprayed coatings, J. Mater. Sci. 27 (1992) 5591–5596.
[9] P.D. Harmsworth, R. Stevens, Microstructure and phase composition of $ZrO_2–CeO_2$ thermal barrier coatings, J. Mater. Sci 26 (1991) 3991–3995.
[10] J.W. Holmes, B.H. Pilsner, Cerium oxide stabilized thermal barrier coatings: Thermal spray, advances in coatings technology, Proceedings of NTSC, 14–17 September, 1987, FL, USA, pp. 259–270.
[11] P. Scardi, E. Galvanetto, A. Tomasi, L. Bertamini, Thermal stability of stabilized zirconia thermal barrier coatings prepared by atmosphere- and temperature-controlled spraying, Surface and Coatings Technology 68/69 (1994) 106–112.

[12] S. Meriani, Features of the caeria–zirconia system, Mater. Sci. And Engg, A 109 (1989) 121–130.
[13] S. Stecura, New ZrO_2–Yb_2O_3 plasma sprayed coatings for thermal barrier applications, Thin solid films 150 (1987) 15–40.
[14] H.L. Tsai, P.C. Tsai, D.C. Tu, Characterization of laser glazed plasma sprayed yttria stabilized coatings, Mater. Sci. And Engg. A 161 (1993) 145–155.
[15] P. Ramaswamy, S. Seetharamu, K.B.R. Varma, K.J. Rao, A simple method for the preparation of plasma-sprayable powders based on ZrO_2, J. Mater. Sci. 31 (1996) 6325–6332.
[16] A.H. Heuer, M. Ruhle, Phase transformations in ZrO_2-containing ceramics I: the instability of c-ZrO_2 and the resulting diffusion controlled reactions, in: N. Claussen, M. Ruhle, A.H. Heuer (Eds.), Science and Technology of Zirconia II, Advances in Ceramics, Vol. 12, ACS, Columbus, OH, USA, 1984, pp. 1–13.
[17] M. Ruhle, A.H. Heuer, Phase transformations in ZrO_2-containing ceramics II: the martensitic reaction in t-ZrO_2, in: N. Claussen, M. Ruhle, A.H. Heuer (Eds.), Science and Technology of Zirconia II, Advances in Ceramics, Vol. 12, ACS, Columbus, OH, USA, 1984, pp. 14–32.
[18] R.C. Garvie, P.S. Nicholson, Structure and thermomechanical properties of partially stabilized zirconia in the CaO–ZrO_2 system, J. Amer. Cer. Soc. 55(3) (1972) 152–157.
[19] J.R. Brandon, R. Taylor, Phase stability of zirconia-based thermal barrier coatings, part II—zirconia–ceria alloys, Surface and coatings technology 46 (1991) 91–101.
[20] B.C. Wu, E. Chang, S.F. Chang, D. Tu, Degradation mechanisms of ZrO_2–8 wt% Y_2O_3/Ni—22Cr–10Al–1Y thermal barrier coatings, J. Amer. Cer. Soc. 72(2) (1989) 212–218.
[21] B.C. Wu, E. Chang, C.H. Chao, M.L. Tsai, The oxide pegging spalling mechanism and spalling modes of ZrO_2 8 wt% Y_2O_3/Ni–22Cr–10Al–1Y thermal barrier coatings under various operating conditions, J. Mater. Sc. 25 (1990) 1112–1119.
[22] R.A. Miller, Oxidation-based model for thermal barrier coating life, J. Amer. Cer. Soc. 67(8) (1984) 517–521.
[23] W.D. Kingery, H.K. Bowen, D.R. Uhlmann, Introduction to Ceramics, Wiley, New York, 1976, (Chapter 14).